# 3,5,3 ',4 ',5 '-Pentamethoxystilbene (MR-5), a Synthetically Methoxylated Analogue of Resveratrol, Inhibits Growth and Induces G1 Cell Cycle Arrest of Human Breast Carcinoma MCF-7...

**ARTICLE** *in* JOURNAL OF AGRICULTURAL AND FOOD CHEMISTRY · NOVEMBER 2009

Impact Factor: 2.91 · DOI: 10.1021/jf903067g · Source: PubMed

DOI:10.1021/jf903067g

JOURNAL OF AGRICULTURAL AND FOOD CHEMISTRY
ARTICLE

# 3,5,3′,4′,5′-Pentamethoxystilbene (MR-5), a Synthetically Methoxylated Analogue of Resveratrol, Inhibits Growth and Induces G1 Cell Cycle Arrest of Human Breast Carcinoma MCF-7 Cells

Min-Hsiung Pan,[†] Chih-Li Lin,[§] Jie-Heng Tsai,[#] Chi-Tang Ho,[⊥] and Wei-Jen Chen*,[#]

[†]Department of Seafood Science, National Kaohsiung Marine University, No. 142 Hai-Chuan Road, Nan-Tzu, Kaohsiung 811, Taiwan, [§]Institute of Medicine and Department of Medical Research, Chung Shan Medical University Hospital, No. 110, Section 1, Chien-Kuo N. Road, Taichung 402, Taiwan, [#]Department of Biomedical Sciences and Department of Medical Research, Chung Shan Medical University Hospital, No. 110, Section 1, Chien-Kuo N. Road, Taichung 402, Taiwan, and [⊥]Department of Food Science, Cook College, Rutgers University, New Brunswick, New Jersey 08901-8520

3,5,3′,4′,5′-Pentamethoxystilbene (MR-5) is a synthetically methoxylated analogue of resveratrol and has been suggested to have antitumor activity because of structural similarity to resveratrol. Herein, we investigate the antiproliferative effect of MR-5 in human breast cancer MCF-7 cells and demonstrate that MR-5 had a more potent inhibition on cell growth compared with resveratrol and other methoxylated derivatives. Exploring the growth-inhibitory mechanisms of MR-5, we found that it is accompanied by G1 cell cycle arrest, which coincides with a marked inhibition of G1 cell cycle regulatory proteins, including decreased cyclins (D1/D3/E) and cyclin-dependent kinases (CDK2/4/6) and increased CDK inhibitors (CKIs) such as p15, p16, p21, and p27. Furthermore, the increase in CKI levels by MR-5 resulted in a concomitant increase in their interactions of CDK4 and CDK2, along with a strong inhibition in CDK4 kinase activity and the accumulation of hypophosphorylated Rb. MR-5 also modulated some critical kinase activities related to cell cycle regulation, including Akt, mitogen-activated protein kinase (ERK1/2), p38 mitogen-activated protein kinase (p38 MAPK), and focal adhesion kinase (FAK) in MCF-7 cells. In total, our results demonstrate that MR-5 affects multiple cellular targets that contribute to its antiproliferative activity in MCF-7 cells and provide novel information for synthetic chemists to design new antitumor agents with introduction of methoxylated group(s) in the basic compound.

**KEYWORDS: 3,5,3′,4′,5′-Pentamethoxystilbene (MR-5); resveratrol; cell cycle; G1 arrest; cyclins; cyclin-dependent kinases (CDKs); CDK inhibitors (CKIs)**

## INTRODUCTION

Resveratrol (3,5,4′-trihydroxystilbene, **Figure 1**) is a natural stilbene-based antioxidant present in various plants including grapes, peanuts, and berries (*1*); it has acquired more attention because of its health benefits. It was not until 1997 that resveratrol was suggested as a potential cancer preventive agent, which blocked carcinogen-induced prenoeplastic lesions in mouse mammary culture and inhibited tumorigenesis in a mouse skin cancer model (*2*). Numerous studies have described the cancer preventive mechanisms of resveratrol. For example, resveratrol was shown to inhibit the activity and expression of cytochrome P450 1A1 (CYP1A1), a phase I enzyme, which are required for activation of carcinogens or mutagens (*3*, *4*). Resveratrol was further shown to induce phase II enzymes such as UDP-glucuronyltransferase and NAD(P)H:quinine oxidoreductase in mouse epidermis, which are responsible for conjugation/detoxification of the activated carcinogens (*5*). Moreover, resveratrol was also reported to have growth-inhibitory effects on different cancerous and transformed cell lines by arresting cell cycle progression or inducing apoptosis (*6*, *7*) and to decrease implanted tumor growth in a rat tumor model (*8*). These diverse antitumor activities of resveratrol make it a lead compound for the development of new effective cancer therapeutic or preventive agents (*9*).

Aberrant control of cell cycle is a result of cancer development (*10*). In mammalian cells, cell cycle progression is stringently regulated by a series of cyclin-dependent kinases (CDKs), cyclins, and CDK inhibitors (CKIs) that drive cell cycle progression through the phosphorylation and dephosphorylation of several regulatory proteins at G1/S checkpoint and G2/M

*Address correspondence to this author at the Department of Biomedical Sciences, Chung Shan Medical University, and Department of Medical Research, Chung Shan Medical University Hospital, No. 110, Section 1, Chien-Kuo N. Road, Taichung 402, Taiwan [telephone (886)-4-24730022 ext.11808; fax (886)-4-23248187; e-mail cwj519@csmu.edu.tw].

 Published on Web 11/16/2009 

checkpoint. (*11*). In early G1 phase, the D-type cyclin accumulates in nucleus in response to mitogenic signaling and then assembles with CDK4/6 to form complexes, which lead to the initial phosphorylation of the retinoblastoma (Rb) family of proteins. When cell cycle enters into late G1 phase, the E-type cyclin forms a complex with CDK2 to facilitate the phosphorylation and, consequently, inactivation of Rb proteins, thus relieving the E2F transcription factor and allowing the G1 cells to enter the S phase. The full CDK activity is modulated by the phosphorylation of CDK on a conserved threonine residue (*12*) or by binding to CKIs . CKIs can be divided into two families, including the Ink4 family (p15, p16, p18, and p19) and the Cip/Kip family (p21, p27, and p57) (*13*). The Ink4 proteins bind to CDK4/6 and thereby block the formation of CDK4/6-cyclin complexes. The high levels of Cip/Kip proteins inhibit CDK2 activity, presumably by increasing the stoichiometry in the CDK2 complexes (*13*). However, these G1/S-associated regulators are frequently mutated and deregulated in various human cancers, and the main disorders include overexpression of D-type cyclins, hyperactivation of CDK4/6 kinases, and functional loss of CKIs and Rbs (*10*, *14*). These observations suggest that impairment in the regulation of G1/S transition may be one of the most common causes of neoplastic transformation. A recent study reports that ablation of cyclin D1 (and hence CDK4 activity) prevents breast cancer development driven by *ErbB2* and *H-ras* oncogenes in a mouse tumor model (*15*), suggesting that targeting chaotic G1-cell cycle regulators may be an effective strategy for possible therapeutic intervention of cancers.

Previously, with the goal of acquisition of a novel resveratrol analogue with more potential antitumor activity, the hydroxyl groups at the stilbene scaffold of resveratrol were manipulated to generate a series of novel methoxylated derivatives of resveratrol.

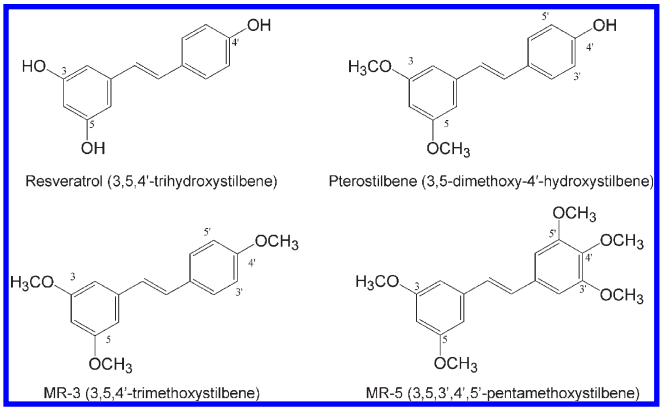


**Figure 1.** Chemical structures of resveratrol and its methoxylated analogues.

Among the tested analogues, we have demonstrated that 3,5,4′-trimethoxystilbene (MR-3, **Figure 1**) was more effective than resveratrol in blocking human colorectal carcinoma cell growth and suggested the importance of the 3,5,4′-trimethoxy motif in conferring antiproliferative activity (*16*). Herein, we aim to assess and compare the antineoplastic capacity of 3,5,3′,4′,5′-pentamethoxystilbene (MR-5, **Figure 1**), the other methoxylated analogue of resveratrol, with those of resveratrol and its methoxylated derivatives, using human breast cancer cell line MCF-7. We first evaluated the superiority of the antitumor effects of these structurally related compounds. Then we characterized the molecular mechanisms involved in MR-5-induced growth inhibition by determining cell cycle distribution and the expression, interaction, and activity of a number of cell cycle regulatory proteins. Finally, the effects of MR-5 on the activation of several kinases critically responsible for cell proliferation were also explored. The present study provides novel evidence that MR-5 may be a potently cancer chemopreventive agent against some types of breast carcinomas.

## MATERIALS AND METHODS

**Materials.** Resveratrol was synthesized using 4-methoxybenzyl alcohol and 3,5-dimethoxybenzaldehyde as precursors as described before (*17*). A similar approach was applied to synthesize its methoxylated derivatives including pterostilbene, MR-3, and MR-5. The purity of these compounds is >97−99% by HPLC or GC. Propidium iodide and RNaseA were available from Sigma (St. Louis, MO). RT-PCR reagents were from Promega (Madison, WI). The antibody against HSP-90 was obtained from Santa Cruz Biotechnology (Santa Cruz, CA). Antibodies against phospho-p38 MAPK (Thr180/Tyr182), p38, phospho-ERK1/2 (Thr42/Tyr44), ERK1/2, phospho-Akt (Ser473), Akt, and all G1 cell cycle regulators were from Cell Signaling Technology (Beverly, MA). Phospho-FAK (Tyr397) and FAK antibodies were purchased from BD Biosciences (San Diego, CA).

**Cell Culture.** Monolayer cultures of human breast carcinoma MCF-7 cells obtained from American Type Culture Collection (ATCC) were grown in Dulbecco's minimal essential medium (DMEM) supplemented with 10% fetal calf serum (Gibco BRL, Grand Island, NY), 100 units/mL of penicillin, and 100 μg/mL of streptomycin and kept at 37 °C in a humidified atmosphere of 5% $CO_2$ in air according to ATCC recommendations. For all experiments, the cells were subjected to no more than 20 passages.

**Lymphocyte Isolation and Culture.** The venous whole blood obtained from a healthy donor was diluted 1:3 with PBS for centrifugation at 1500 rpm at room temperature for 10 min. The samples were carefully layered over Ficoll Hypaque (Pharmacia, Uppsala, Sweden) followed by centrifugation at 3000 rpm at room temperature for 15 min. Peripheral blood mononuclear cells (PBMCs) were isolated and adjusted to $1 \times 10^6$ cells/mL of RPMI complete medium with 10% fetal calf serum. Then PBMCs were cultivated at 37 °C in a humidified atmosphere containing 5% $CO_2$.

**Table 1.** Primer Sequences and Their Annealing Conditions Used for RT-PCR[a]

| name/Genbank accession no. | sequence (5′ → 3′) | cycles | annealing temp/time |
|---|---|---|---|
| *Homo sapiens* cyclin-dependent kinase inhibitor 2B (**p15**)/NM_004936.3 | forward: ggcagtcgatgcgttcactc<br>reverse: cagggcttccagagagtgtc | 30 | 55 °C/45 s |
| *Homo sapiens* cyclin-dependent kinase inhibitor 2A (**p16**)/ NM_058195.2 | forward: gcgatgtcgcacggtacctg<br>reverse: gggcagttgtggccctgtag | 30 | 56 °C/45 s |
| *Homo sapiens* cyclin-dependent kinase inhibitor 1B (**p27**)/ NM_004064.3 | forward: cagactcggacgggctttg<br>reverse: acggcccgagctctaggag | 30 | 56 °C/60 s |
| *Homo sapiens* glyceraldehyde-3-phosphate dehydrogenase (**GAPDH**)/ NM_002046.3 | forward: tgaaggtcggtgtgaacggatttggc<br>reverse: catgtaggccatgaggtccaccac | 30 | 55 °C/30 s |

[a] The *GAPDH* gene was used as an internal standard to normalize the amount of total RNA present in each reaction.

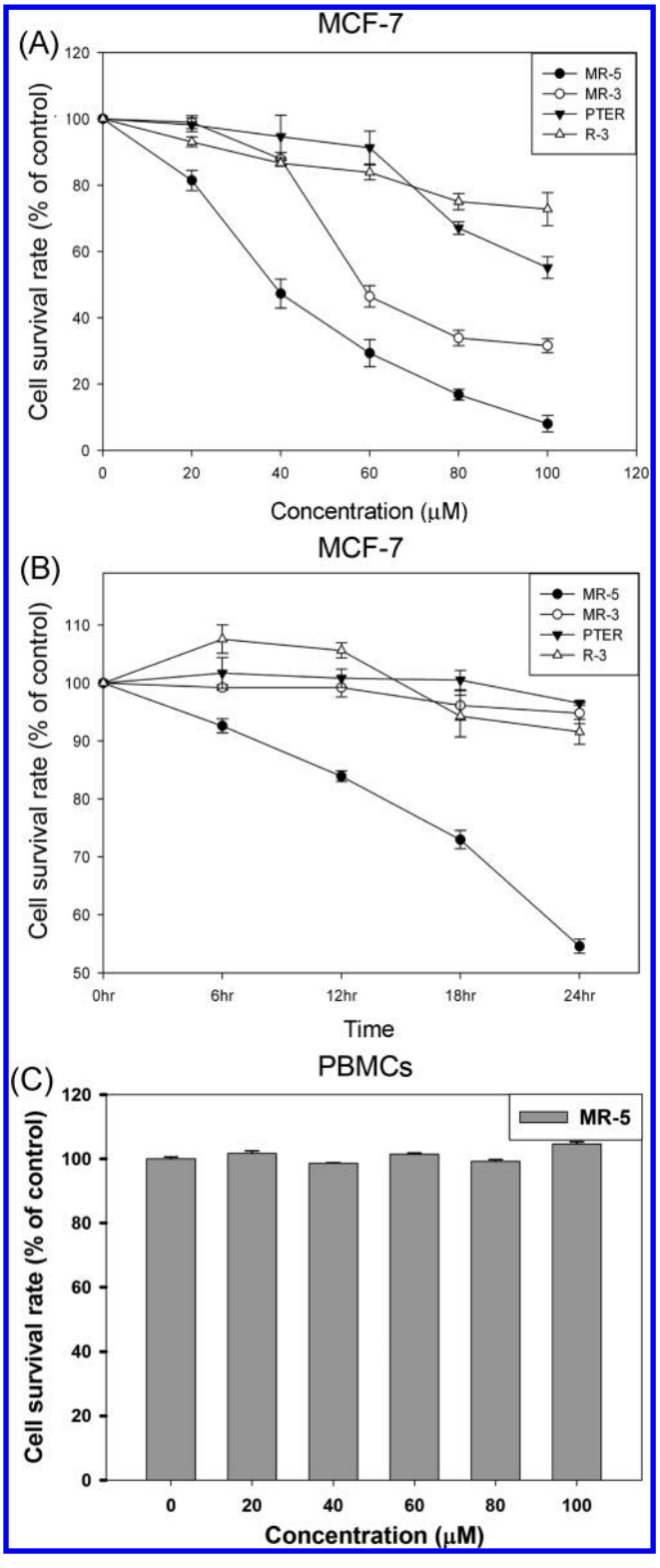


**Figure 2.** (**A**, **B**) Effect of resveratrol and its methoxylated derivatives on cell viability of MCF-7 cells. Cells were treated with 0, 20, 40, 60, 80, or 100 $\mu$M concentrations of the indicated resveratrol-related compounds for 24 h (**A**) or with a 30 $\mu$M concentration of these compounds for the indicated times (**B**). (**C**) Cytotoxicity effects of MR-5 on PBMCs. Human lymphocyte cells were treated with 20−100 $\mu$M concentrations of the indicated MR-5 for 24 h. Cell viability was then determined by MTT assay as described under Materials and Methods. The percentage of cell viability was calculated as the ratio (A570) of treated cells to control cells. Data represent the mean ± SE of three independent experiments. R-3, resveratrol; PTER, pterostilbene; MR-3, 3,5,4′-trimethoxystilbene; MR-5, 3,5,3′,4′,5′-pentamethoxystilbene.

**Cell Viability Assay.** The cells were seeded at a density of $5 \times 10^3$ cells/mL into 96-well plates and grown overnight. Then the cells were treated with various concentrations of resveratrol, pterostilbene, MR-3, or MR-5 for the indicated times. All of these compounds used were dissolved in DMSO. Control cells were treated with DMSO to yield a final contration of 0.05% (v/v). After incubation, the proliferating cell numbers were determined by the MTT (3-(4,5-dimethylthiazol-2-yl)-2,5-diphenyltetrazolium bromide) assay as follows: 20 $\mu$L of MTT solution (5 mg/mL, Sigma) was added to each well and incubated for 24 h at 37 °C. Then the supernatant was aspirated, and the MTT−formazan crystals formed by metabolically viable cells were dissolved in 200 $\mu$L of dimethyl sulfoxide (DMSO). Finally, the absorbance was monitored by a microplate reader at a wavelength of 570 nm.

**Soft Agar Assay.** Single-cell suspensions of MCF-7 cells were treated with 0, 15, or 30 $\mu$M MR-5 and then mixed with agarose in a final concentration of 0.35%. Aliquots of 1.5 mL containing $1 \times 10^4$ cells with 10% FCS were plated in triplicate in 6 cm culture dishes over a base layer of 0.7% agarose and allowed to grow. Colonies of > 60 mm were counted after 14 days of incubation.

**Cell Cycle Analysis.** Cell cycle distribution was analyzed by flow cytometry as follows. After treatment of MR-5, cells were harvested, washed twice with phosphate-buffered saline (PBS), and fixed in 70% ethanol for at least 2 h at −20 °C. Fixed cells were washed with PBS, incubated with 1 mL of PBS containing 0.5 $\mu$g/mL RNase A and 0.5% Triton X-100 for 30 min at 37 °C, and then stained with 50 $\mu$g/mL propidium iodide. The stained cells were analyzed using a FAScan laser flow cytometer equipped with Cell Quest software (Becton Dickinson, San Jose, CA).

**Western Blotting (Immunoblotting).** Total protein extracts were prepared in a lysis buffer (50 mM Tris-HCl, pH 8.0, 5 mM EDTA, 150 mM NaCl, 0.5% NP-40, 0.5 mM phenylmethanesulfonyl fluoride, and 0.5 mM dithiothreitol) for 30 min at 4 °C. Equal amounts of total cellular proteins (50 $\mu$g) were resolved by sodium dodecyl sulfate−polyacrylamide gel electrophoresis (SDS-PAGE), transferred onto polyvinylidene difluoride (PVDF) membranes (Immobilon P, Millipore, Bedford, MA), and then probed with primary antibody followed by secondary antibody conjugated with horseradish peroxidase. The immunocomplexes were visualized with enhanced chemiluminescence kits (Amersham, U.K.).

**Immunoprecipitation.** One hundred microliter of cell lysate (containing 500 $\mu$g total cellular proteins) was first precleared by being incubated with protein A−agarose (10 $\mu$L, 50% slurry, Santa Cruz Biotechnology) for 15 min. The clarified supernatants were collected by microfugation and then incubated with primary antibody for 2 h at 4 °C. The reaction mixtures were amended with 20 $\mu$L of protein A−agarose to absorb the immunocomplexes at 4 °C overnight. Immunoprecipitated proteins were subjected to SDS-PAGE and then transferred onto a PVDF membrane (Millipore). The resulting proteins were visualized by immunoblotting.

**Reverse Transcription Polymerase Chain Reaction (RT-PCR).** Total RNA was isolated using TRIzol reagent (Sigma) as recommended by the manufacturer's instructions. Briefly, total RNA (5 $\mu$g) was reverse-transcribed into cDNA using Moloney murine leukemia virus (M-MLV) reverse transcriptase and oligo (dT) 18 primer by incubating the reaction mixture (25 $\mu$L) at 40 °C for 90 min. Amplification of cDNA was performed by PCR in a final volume of 50 $\mu$L containing 2 $\mu$L of RT product, dNTPs (each at 200 $\mu$M), 1× reaction buffer, a 1 $\mu$M concentration of each primer, and 50 units/mL Pro Taq DNA polymerase. The specific PCR primers used in this experiment, and the temperature and incubation time of annealing for each primer pairs, are listed in **Table 1**. After an initial denaturation for 5 min at 95 °C, 30 cycles of amplification (denaturation at 95 °C for 30 s and extension at 72 °C for 1 min) were performed, followed by 72 °C for 10 min. A 5 $\mu$L sample of each PCR product was electrophoresed on a 2% agarose gel and visualized by ethidium bromide staining. Each value was normalized to the expression of GAPDH. Values presented are the means ± SE of triplicate measurements.

**In Vitro CDK4 Kinase Assay.** CDK4 kinase activity was determined by an in vitro method (*18*). Briefly, 500 $\mu$g of total proteins from cell lysates was precleared with protein A−agarose, and CDK4 protein was then immunoprecipitated using anti-CDK4 antibody with protein A−agarose

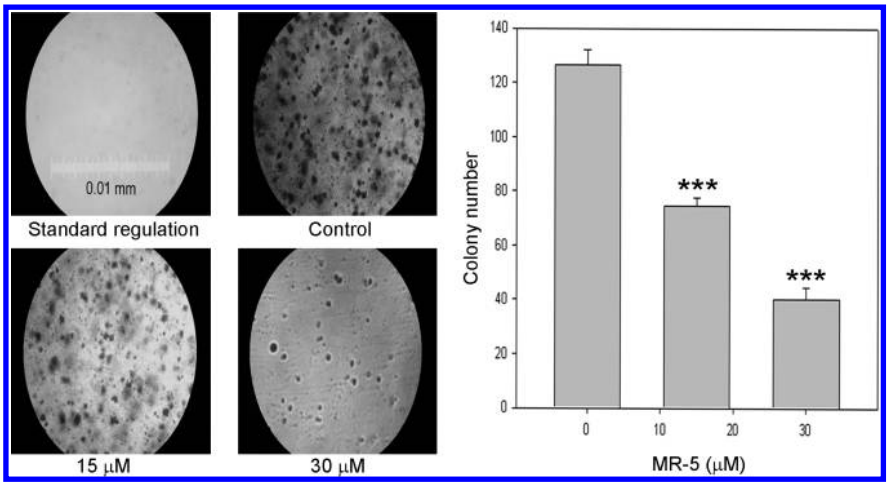


**Figure 3.** Colony formation in soft agar. MCF-7 cells were seeded into a 0.35% soft agar in DMEM containing 1% FCS over 0.7% agarose in 6 cm dishes to test colony formation with treatment of MR-5 (15 and 30 $\mu$M) or not (control). Colony size and number were determined by microscopy after 14 days of incubation at 37 °C in 5% $CO_2$. For quantification, colonies >60 mm were scored, and statistical analysis was analyzed by *t* test. Asterisks represent statistically significant differences compared to the control group (***, $p < 0.001$).

beads. After overnight incubation at 4 °C, the immunocomplexes were washed three times with washing buffer containing 50 mM HEPES−KOH, pH 7.5, 150 mM NaCl, 1 mM EDTA, 2.5 mM EGTA, 1 mM DTT, 80 mM $\beta$-glycerophosphate, 1 mM NaF, 0.1 mM sodium orthovanadate, 0.1% Tween 20, 10% glycerol, 1 mM PMSF, and 10 $\mu$g/mL aprotinin and leupeptin and rinsed with kinase buffer containing 50 mM HEPES−KOH, pH 7.5, 2.5 mM EGTA, 1 mM DTT, 10 mM $\beta$-glycerophosphate, 10 mM $MgCl_2$, 1 mM NaF, and 0.1 mM sodium orthovanadate. Rb phosphorylation was determined by incubating the immunocomplexes with 30 $\mu$L of Rb kinase solution containing 1 $\mu$g of Rb substrate protein (Santa Cruz Biotechnology) and 0.1 mM ATP in kinase buffer for 30 min at 37 °C. Then, the phosphorylated Rb was subjected to SDS-PAGE, transferred, and then visualized by immunoblotting with antibodies against specific phosphorylated sites of Rb substrate.

**Statistical Analysis.** Quantitative data represent mean values with the respective standard error of the mean (SE) corresponding to three or more replicates. Data were analyzed by one-way analysis of variance (ANOVA) using post hoc multiple comparison Tukey's b. Data were considered to be statistically significant at $p < 0.05$.

## RESULTS

**Inhibition of Cell Growth of Human Breast Carcinoma Cells by MR-5.** We first compared the effects of resveratrol and its methoxylated analogues including pterostilbene (*trans*-3,5-dimethoxy-4′-hydroxystilbene), MR-3 (3,5,4′-trimethoxystilbene), and MR-5 (**Figure 1**) on the growth of MCF-7 human breast cancer cells using the MTT assay as previously described. As shown in **Figure 2A**, resveratrol and its derivatives exhibited cytotoxic effects on MCF-7 cell growth in a concentration-dependent manner; the $IC_{50}$ value of MR-3 was ~58.4 $\mu$M. However, MR-5 was more effective than resveratrol and other methoxylated analogues as a chemopreventive agent against MCF-7 cells, with an $IC_{50}$ value of ~37.8 $\mu$M. MR-5 also showed a more potent time-related inhibition on MCF-7 cell growth compared with treatment of resveratrol, pterostilbene, or MR-3 (**Figure 2B**). To further determine the effect of MR-5 on normal cells, peripheral blood mononuclear cells (PBMCs) prepared from Ficoll Hypaque separation were subjected to the MTT assay with MR-5 treatment. **Figure 2C** shows that the growth of PBMCs was not inhibited by MR-5, even at the highest concentration of MR-5 (100 $\mu$M), whereas MR-5 suppressed the growth of MCF-7 cells by ~88% at the same concentration. This observation suggested that MR-5 may have potential in chemoprevention. Selectivity of MR-5 against carcinoma cells led to further examination on the mechanism of the antiproliferative effect of MR-5 in MCF-7 cells.

**Inhibition of Colony Formation of MCF-7 Cells on Soft Agar by MR-5.** To investigate the inhibitory effect of MR-5 on cellular transformation in vitro, MCF-7 cells were seeded on soft agar, and transformed colonies > 60 $\mu$m were counted. After 2 weeks of incubation, MR-5 treatment resulted in a decrease in colony formation of MCF-7 cells on soft agar with a lower number of colonies formed and a reduced colony size in a concentration-responsive manner (**Figure 3**). These results suggested that MCF-7 cells lost the capacity of anchorage-independent growth via growth inhibition by MR-5.

**Blockage of Cell Cycle Progression at G1 Phase of MCF-7 Cells by MR-5.** To determine whether the growth inhibition of MCF-7 cells was due to the blockade of cell cycle progression by MR-5, MCF-7 cells treated with DMSO (vehicle control) or MR-5 were subjected to flow cytometric analysis. As shown in **Figure 4A**, MR-5 caused G1 cell cycle arrest in a dose-dependent manner, and MR-5 at 30 $\mu$M reached the highest G1 phase arrest by a significant ~15.79% difference in G1 cells compared with DMSO control. **Figure 4B** also displays that the treatment of MR-5 at 30 $\mu$M in MCF-7 cells gradually caused the accumulation of G1 cells accompanied with the decrease in S and G2/M cells from 6 to 24 h. These results indicated that MR-5 induced cell cycle arrest at G1 in MCF-7 cells, and this effect might consequently cause the growth inhibition of MCF-7 cells.

**Effect of MR-5 on the Expression of G1 Cell Cycle Checkpoint-Related Proteins in MCF-7 Cells.** On the basis of the results of cell cycle distribution, we next investigated whether the cell cycle arrest at G1 phase by MR-5 was related to the expression of cell cycle-regulatory proteins such as cyclin D, cyclin E, and their associated CDK4/6 and CDK2, which are essential for cell cycle progression from G1 to S phase. MCF-7 cells were treated with 30 $\mu$M MR-5 over a 24 h period and then harvested for immunoblotting. As demonstrated in **Figure 5A**, MR-5 markedly down-regulated the protein levels of cyclin D1, D3, CDK4, and CDK6, which are responsible for cell cycle progression in early G1 phase, in a time-responsive manner. We subsequently determined the effect of MR-5 on the protein expression of cycle E and CDK2, which regulate S phase entry in late G1 phase. **Figure 5B** exhibits that MR-5 treatment gradually reduced the protein level of cyclin E from 6 to 24 h, as well as its effects on the levels of cyclin D1/D3 and CDK4/6, whereas there was a slight decrease in the level of

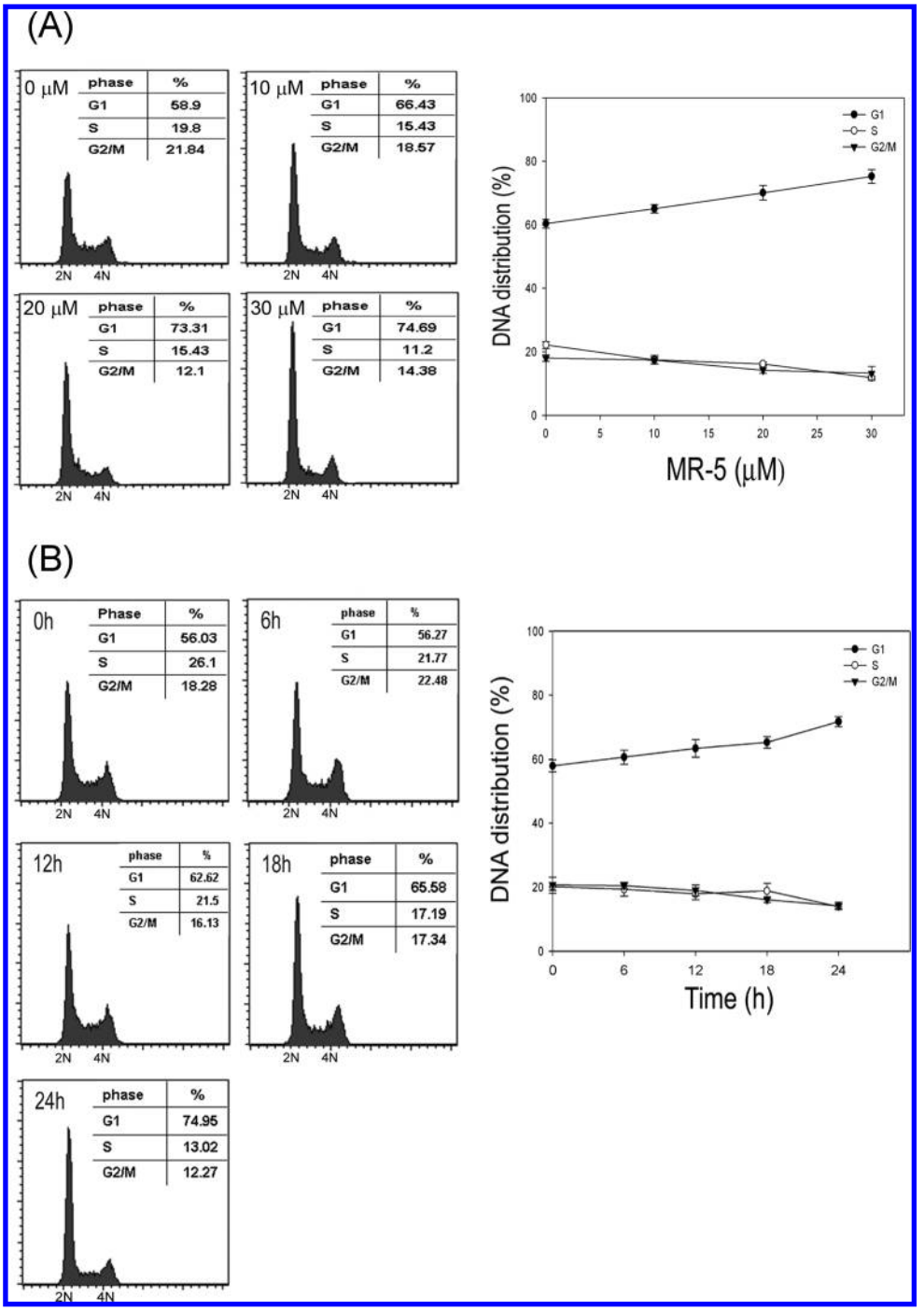


**Figure 4.** Effect of MR-5 on cell cycle of MCF-7 cells. The cultured cells were treated with 10, 20, or 30 $\mu$M MR-5 for 24 h (**A**) or with 30 $\mu$M MR-5 for 6, 12, 18, and 24 h (**B**). After incubation, the cells were harvested by a brief incubation with trypsin−EDTA followed by cell cycle analysis, as detailed under Materials and Methods. For quantification, each experiment was independently performed three times and expressed as the mean ± SE.

CDK2 by MR-5 under the same treatment after 24 h. These results indicate that down-regulation of cyclins and CDKs might be involved in the MR-5-mediated growth arrest in MCF-7 cells.

**Effect of MR-5 on the Phosphorylation Status of Rb Protein in Cultured Cells.** The phosphorylation of Rb protein mediated by cyclin D-Cdk4/6 and cyclin E-Cdk2 kinase complexes is required for the cells to progress from G1 to S phase. To elucidate whether the suppressive expression of cyclins and CDK4/6 by MR-5 can result in the dephosphorylation of Rb protein, the phosphorylation status of Rb was examined following exposure of exponentially growing MCF-7 cells to MR-5 by immunoblotting using specific antibodies against the phosphorylation sites in Rb. **Figure 5C** shows that the degrees of Rb phosphorylation at Ser780, 807, and 811 were down-regulated by MR-5 treatment, beginning at 6 h and up to 24 h, which are associated with a suppressing effect on the levels of cyclin D1/D3/E and CDK4/6 (**Figure 5A**,**B**). These results support our hypothesis that MR-5 blocks cell cycle progression from G1 to S phase by down-regulation of cyclins (cyclins D1, D3, and E) and CDKs (CDK4 and CDK6).

**Up-regulation of CKIs following MR-5 Treatment in MCF-7 Cells.** Cyclin-dependent kinase inhibitors (CKIs) are well characterized to block cell cycle progression by binding and inhibiting CDKs alone or cyclin/CDK complexes. To determine whether

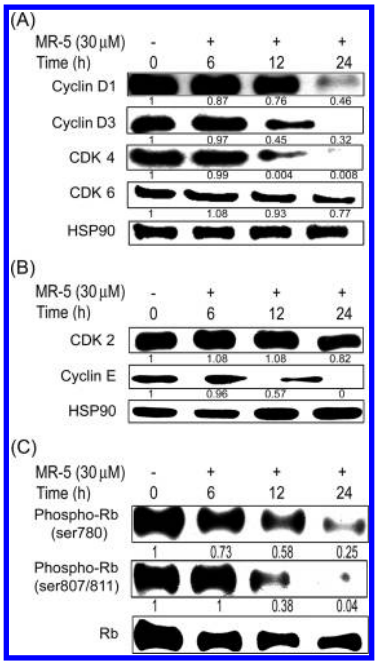


**Figure 5.** Effect of MR-5 on cell cycle-regulated proteins involved in G1 phase progression: (**A**) relative protein levels of cyclin D1, D3, CDK4, and CDK6 involved in early G1 phase regulation; (**B**) protein levels of cyclin E and CDK2 expressed during late G1 phase; (**C**) phosphorylation status of the Rb protein. Cells were treated with 30 $\mu$M MR-5 for the indicated times. At the end of incubation, total proteins in cellular extracts were collected and assayed by Western blotting using antibodies against G1 cell cycle regulators as indicated. Heat shock protein 90 (HSP90) was an internal control for equivalent protein loading. The total and phosphorylated forms of Rb were detected by Western blotting with specific antibodies for each.

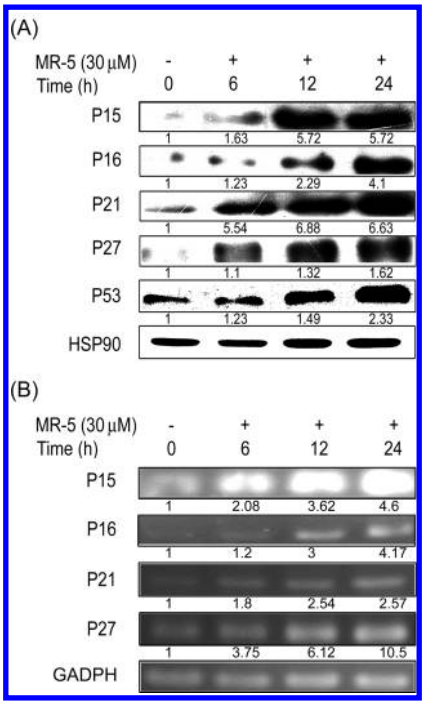


**Figure 6.** Effect of MR-5 on the expression of CKIs in MCF-7 cells. Cells were treated with 30 $\mu$M MR-5 for the indicated times, and (**A**) alteration of the protein levels of CKIs including p15, p16, p21, and p27 by MR-5 were determined by Western blotting with specific antibodies, respectively. Effect of MR-5 on the protein expression of *p53* tumor suppressor gene was also assessed. HSP90 acted as a loading control. (**B**) Effect of MR-5 on mRNA expression of CKIs (p15, p16, p21, and p27). Total RNA was harvested from MR-5-treated MCF-7 cells at the indicated times as described above, and the relative amounts of target mRNA were assessed by RT-PCR. Glyceraldehyde-3-phosphate dehydrogenase (GAPDH) cDNA was used as an internal control.

growth inhibition by MR-5 was related to induce the expression of CKIs, we incubated MCF-7 cells with 30 $\mu$M MR-5 over a 24 h period and then determined the protein levels of CKI members including p15, p16, p21, and p27 by immunoblotting. As shown in **Figure 6A**, MR-5 markedly elevated the expression of all these CKI proteins in a time-dependent manner. The expression of p21 has been reported to be up-regulated by either a p53-dependent or p53-independent mechanism (*19*, *20*). To further demonstrate whether the elevated level of p21 in response to MR-5 was tightly correlated with the status of p53, we examined the level of p53 in MR-5-treated MCF-7 cells by immunoblotting. MR-5 treatment also increased the time-responsive accumulation in p53, and this result was concomitant with the increase in p21 (**Figure 6A**). According to these results, we suggested that the induction of p21 by MR-5 is due to transcriptional regulation by p53.

We were now interested in determining whether the level of the mRNAs encoding p15, p16, p21, and p27 changed and whether these changes were reflected at the protein level. To this end, we checked the mRNA expression of these CKIs following MR-5 treatment by means of RT-PCR. As shown in **Figure 6B**, the mRNAs encoding these CKI proteins apparently increased as well as their protein levels over the 6−24 h treatment with MR-5. These results suggested that the induction of steady-state levels of these CKIs by MR-5 might stem from transcriptional regulation of these proteins.

**Effect of MR-5 on Cyclin/CDK-Associated CKIs and CDK4 Kinase Activity in MCF-7 Cells.** Although MR-5 suppressed expression of cyclin D1/D3/E and CDK4/6 accompanied the induction of p15, p16, p21, and p27, we were not certain of the relationship between cyclin/CDK complexes and their related CKIs following MR-5 treatment. Therefore, we carried out a coimmunoprecipitation to determine the interaction of these cell cycle-regulated factors. The cell extracts from MR-5-treated MCF-7 cells were immunoprecipitated by anti-CDK4 or -CDK2 antibody and then subjected to immunoblotting. As shown in **Figure 7A**, MR-5 gradually enhanced the binding of p15, p16, p21, or p27 to CDK4 with increasing time. On the contrary, MR-5 induced a time-dependent decrease in the levels of cyclin D1/CDK4 and cyclin D3/CDK4 complexes. Similarly, the interaction between p27 and CDK2 was also induced by treatment of MR-5 in a time-related manner, accompanied with the decrease in cyclin E/CDK2 complex (**Figure 7B**). These findings implied that up-regulation of the interaction between CDKs and their related CKIs plays a critical role in G1 cell cycle arrest of MCF-7 cells by MR-5. To further assess whether the increased binding of CKIs with CDK would alter the kinase activity of CDK, we performed an in vitro kinase assay and found that MR-5 exerted a time-dependent inhibition in CDK4 kinase activity with a reduction in phosphorylation of Rb substrate at Ser780 and Ser807/811 (**Figure 7C**), supporting the above suggestion.

**Effect of MR-5 on the Activation of Signal Transduction in MCF-7 Cells.** To further determine the action mechanisms underlying MR-5-mediated growth inhibition, relevant over-expressed or activated signaling proteins including phosphotidylinositol 3-kinase (PI3K)-Akt, mitogen-activated protein kinase (ERK1/2), p38 mitogen-activated protein kinase (p38 MAPK), and focal adhesion kinase (FAK) in MCF-7 cells were examined. We performed immunoblotting to detect the phosphorylated degrees of these kinases, which have direct correlation

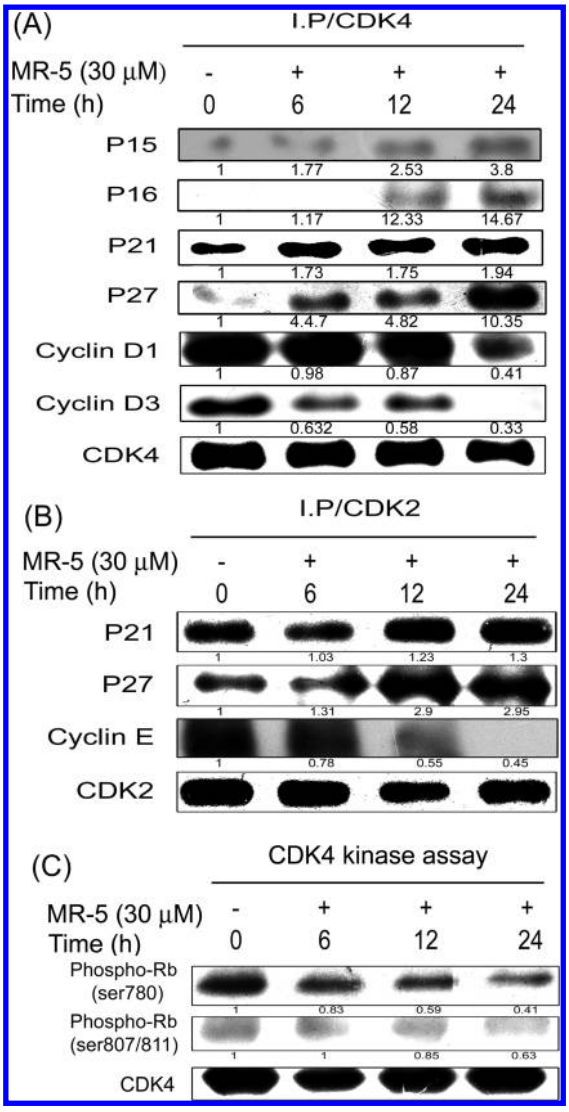


**Figure 7.** Effect of MR-5 on CDK-associated cyclins and CKIs and CDK4 kinase activity in MCF-7 cells. Cells were treated with 30 $\mu$M MR-5 for the indicated times. After incubation, MR-5-treated cell lysates were immunoprecipitated with CDK4 (**A**) or CDK2 (**B**) antibodies and then immunoblotted for antibodies against the related cyclins and CKIs as labeled in the figure, respectively. Each experiment was independently performed three times. For CDK4 kinase activity (**C**), CDK4 was immunoprecipitated from MR-5-treated cell lysates and then subjected to kinase assay in the presence of ATP and Rb substrate protein, as described under Materials and Methods. The phosphoserine sites of Rb substrate at Ser780 and Ser807/811 were determined by Western blotting with the phosphoserine-specific antibodies. IP, immunoprecipitation.

with their activation. As demonstrated in **Figure 8**, MR-5 had a suppressing effect on the phosphorylation of Akt, ERK1/2, and FAK. By contrast, MR-5 time-dependently increased the phosphorylation of p38 MAPK. These results suggested that the inhibitory modification of these kinase signaling pathways by MR-5 may contribute to antiproliferative ability of MR-5 in MCF-7 breast carcinoma cells.

## DISCUSSION

Resveratrol has received widespread attention due to its spectrum of healthy benefits including cancer preventive and therapeutic activities and has been considered as a lead compound regarding the development of new anticancer agents.

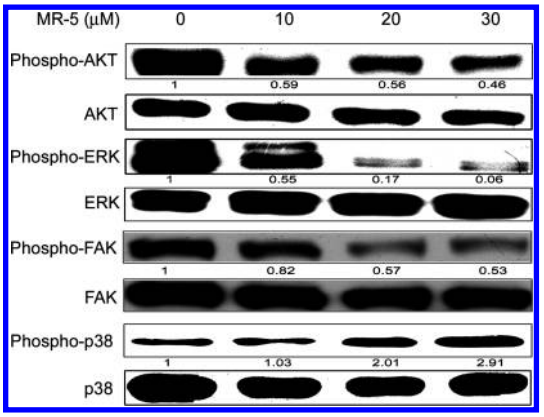


**Figure 8.** Multiple effects of MR-5 on signaling pathways. MCF-7 cells were exposed by treatment of MR-5 with a variety of concentrations for 24 h, and then the resulting lysates were prepared: (**A**) phosphorylated Akt (phospho-Akt), (**B**) phosphorylated ERK1/2 (phospho-ERK), (**C**) phosphorylated p38 MAPK (phospho-38), or (**D**) phosphorylated FAK (phospho-FAK) was determined by Western blotting. The native protein was used as a loading control. The Western blot data presented are representative of those obtained in at least three separate experiments.

Recently, it has been reported that methoxylated derivatives of resveratrol, especially the 3,5-dimethoxy compounds, are more active than natural resveratrol in inducing several human leukemia and lymphoma cells undergoing apoptosis (*21*, *22*). On the basis of this suggestion, pterostilbene, a natural 3,5-dimethoxy analogue of resveratrol (**Figure 1**), was evaluated for its antileukemic capacity and found to be a more effective apoptosis-inducing agent compared to resveratrol in leukemia cells (*21*). Our previous study has also demonstrated that the synthetic resveratrol analogue 3,5,4′-trimethoxystilbene (MR-3, **Figure 1**) was potent against the growth of several human cancer cells and inhibited xenograft tumor growth of colorectal cancer in SCID mice (*16*). These findings suggest that introduction of methoxy groups on the phenyl ring motif of resveratrol might increase the lipophilicity, which endows these methoxylated derivatives with pro-apoptotic or growth-inhibitory activity. With the goal of obtaining more potent anticancer agents, MR-5 was synthesized such that methoxy groups were placed on the 3-, 5-, 3′-, 4′- and 5′-positions of the phenyl rings of resveratrol. As expected, MR-5 has superior antiproliferative effects over resveratrol, pterostilbene, and MR-3 in the order MR-5 > MR-3 > pterostilbene > resveratrol in MCF-7 breast cancer cells in either a dose- or a time-dependent manner (**Figure 2**), consistent with the assumption that the presence and position of methoxy groups at the stilbene-based motif of resveratrol are significant and related to the cytotoxic ability of these corresponding compounds.

Resveratrol was reported to induce a G1 cell cycle arrest with apoptosis in MCF-7 cells (*23*). This raised the possibility that growth inhibition of MR-5 in MCF-7 cells might stem from modulation of cell cycle progression and prompted us to investigate in further detail the mechanism of action of MR-5 on the cell cycle machinery. From an analysis of cell cycle distribution, MR-5 produced a strong inhibition on cell cycle progression and committed cells to G1 arrest (**Figure 4**), accompanied with down-regulation of cyclin D1/D3/E and CDK2/4/6 (**Figure 5**) and up-regulation of CKIs including p15, p16, p21, and p27 (**Figure 6**). An important mechanism for regulating cell cycle progression is controlled by the activity of CDKs, which is regulated by interacting with their respective CDK subunits and CKIs (*11*). Considering the presence of significant levels of CKIs and hypophosphorylation of Rb protein induced by MR-5

in MCF-7 cells, we suggested that MR-5 might also inhibit the G1/S phase transition of the cell cycle via modulation of the binding of CKIs to their responsive cyclin/CDK complexes. In our data, we clearly showed that MR-5 induced a marked increase in the levels of CKIs (p15, p16, p21, and p27), together with their increased binding with CDK4 and CDK2 (**Figure 7A**, **B**); meanwhile, a decrease in the formation of both D-type cyclins/CDK4 and cyclin E/CDK2 complexes and a strong inhibition in CDK4 kinase activity by MR-5 treatment were also observed (**Figure 7**). Therefore, cell cycle control through inducing an increased interaction between induced levels of CKIs with CDKs and consequently inhibiting CDK kinase activity appears to be a relevant mechanism involved in MR-5-induced G1 cell cycle arrest of MCF-7 cells.

It is well-known that cyclin D1 expression is regulated transcriptionally by growth receptor-mediated signaling including ERK1/2- and p38-MAP kinase cascade pathways (*24*). During the G1 phase, activation of the ERK1/2 cascade by mitogen was capable of fully driving cyclin D1 protein expression and, therefore, cdk4/6 activity. In contrast to the ERK1/2 cascade, activation of the p38 MAPK cascade was less sensitive to mitogenic stimuli and shows an antagonistic effect on the regulation of mitogen-induced cyclin D1 expression (*24*). A recent paper described a marked inhibition of the MEK-EEK1/2 signaling pathway, along with the down-regulation of cyclin D1 and CDK6 levels, in A431 epidermoid carcinoma cells treated by resveratrol (50−100 $\mu$M) (*25*). Considering that MR-5 significantly inhibited ERK1/2 and activated p38 MAPK, we suggested that in MCF-7 cells, modulation of these two kinase activities by MR-5 could result in a decrease in D-type cyclin levels, thereby suppressing CDK4/6 activities and G1/S transition.

The cyclin D1 level is also modulated by its degradation. Proteolysis of cyclin D1 is controlled through the ubiquitin−proteosome system following phosphorylation of cyclin D1 at a conserved C-terminal threonine, Thr286, by the glycogen synthase kinase-3$\beta$ (GSK-3$\beta$) (*26*). GSK-3$\beta$ is a crucial component of the PI3K-Akt pathway and negatively regulated by Akt. Akt also indirectly decreases the protein level of p27 by inactivation of the forkhead transcription factors that transcriptionally increase p27 protein expression and consequently result in growth inhibition (*27*). Our result showed that MR-5 has a strong inhibition on Akt activation (**Figure 8**), together with a decreased level of cyclin D1 and an increased level of p27. It is suggested that MR-5 might up-regulate GSK-3$\beta$ activity and thereby accelerate the degradation of cyclin D1 through the proteasome-mediated pathway. MR-5 might also exert a positive effect on the activity of some forkhead transcription factors, resulting in increased protein level of p27.

MR-5 not only blocked MCF-7 cell cycle progression during G1/S transition but also suppressed MCF-7 cells to grow on soft agar (**Figure 3**). Given that anchorage-dependent growth is regulated by integrin-FAK signaling and increased FAK level or activity has been implicated in tumor invasion or metastasis, as reviewed (*28*−*30*), we determined the activation of FAK under MR-5 treatment and found that MR-5 dose-dependently inhibited phosphorylation of FAK at Tyr397, an event involved in integrin receptor firing and enabling cells to grow in an anchorage-dependent fashion (*28*). On basis of these results, we suggested that the reduction of FAK activity by MR-5 might, in part, result in growth inhibition of MCF-7 cells on soft agar, but the detailed mechanisms require further investigation.

To sum up, the current study concludes that MR-5 affects multiple cellular signaling pathways and targets in MCF-7 human breast carcinoma cells and that modulation of G1 cell cycle regulators such as D- and E-type cyclins, CDKs, CKIs, and pRb contributes to its antiproliferative effect on MCF-7 cells. The results also revealed that MR-5 is the most potent suppressor of MCF-7 cell proliferation compared with resveratrol and its methoxylated analogues and imply that introduction of methoxy groups on the basic chemical structure of resveratrol may be an accessible tactic to increase cytotoxicity of these stilbene-based compounds against some types of cancer cells.

## LITERATURE CITED


(1) Burns, J.; Yokota, T.; Ashihara, H.; Lean, M. E.; Crozier, A. Plant foods and herbal sources of resveratrol. *J. Agric. Food Chem.* **2002**, *50*, 3337–3340.

(2) Jang, M.; Cai, L.; Udeani, G. O.; Slowing, K. V.; Thomas, C. F.; Beecher, C. W.; Fong, H. H.; Farnsworth, N. R.; Kinghorn, A. D.; Mehta, R. G.; Moon, R. C.; Pezzuto, J. M. Cancer chemopreventive activity of resveratrol, a natural product derived from grapes. *Science* **1997**, *275* (5297), 218–220.

(3) Chun, Y. J.; Kim, M. Y.; Guengerich, F. P. Resveratrol is a selective human cytochrome P450 1A1 inhibitor. *Biochem. Biophys. Res. Commun.* **1999**, *262* (1), 20–24.

(4) Ciolino, H. P.; Yeh, G. C. Inhibition of aryl hydrocarbon-induced cytochrome P-450 1A1 enzyme activity and CYP1A1 expression by resveratrol. *Mol. Pharmacol.* **1999**, *56* (4), 760–767.

(5) Szaefer, H.; Cichocki, M.; Brauze, D.; Baer-Dubowska, W. Alteration in phase I and II enzyme activities and polycyclic aromatic hydrocarbons-DNA adduct formation by plant phenolics in mouse epidermis. *Nutr. Cancer* **2004**, *48* (1), 70–77.

(6) Fan, E.; Jiang, S.; Zhang, L.; Bai, Y. Molecular mechanism of apoptosis induction by resveratrol, a natural cancer chemopreventive agent. *Int. J. Vitam. Nutr. Res.* **2008**, *78* (1), 3–8.

(7) Kundu, J. K.; Surh, Y. J. Cancer chemopreventive and therapeutic potential of resveratrol: mechanistic perspectives. *Cancer Lett.* **2008**, *269* (2), 243–261.

(8) Carbo, N.; Costelli, P.; Baccino, F. M.; Lopez-Soriano, F. J.; Argiles, J. M. Resveratrol, a natural product present in wine, decreases tumour growth in a rat tumour model. *Biochem. Biophys. Res. Commun.* **1999**, *254* (3), 739–743.

(9) Athar, M.; Back, J. H.; Kopelovich, L.; Bickers, D. R.; Kim, A. L. Multiple molecular targets of resveratrol: anti-carcinogenic mechanisms. *Arch. Biochem. Biophys.* **2009**, *486* (2), 95–102.

(10) Malumbres, M.; Barbacid, M. Cell cycle, CDKs and cancer: a changing paradigm. *Nat. Rev. Cancer* **2009**, *9* (3), 153–166.

(11) Malumbres, M.; Barbacid, M. Mammalian cyclin-dependent kinases. *Trends Biochem. Sci.* **2005**, *30* (11), 630–641.

(12) Kaldis, P. The cdk-activating kinase (CAK): from yeast to mammals. *Cell. Mol. Life Sci.* **1999**, *55* (2), 284–296.

(13) Sherr, C. J.; Roberts, J. M. CDK inhibitors: positive and negative regulators of G1-phase progression. *Genes Dev.* **1999**, *13* (12), 1501–1512.

(14) Freemantle, S. J.; Liu, X.; Feng, Q.; Galimberti, F.; Blumen, S.; Sekula, D.; Kitareewan, S.; Dragnev, K. H.; Dmitrovsky, E. Cyclin degradation for cancer therapy and chemoprevention. *J. Cell Biochem.* **2007**, *102* (4), 869–877.

(15) Yu, Q.; Geng, Y.; Sicinski, P. Specific protection against breast cancers by cyclin D1 ablation. *Nature* **2001**, *411* (6841), 1017–1021.

(16) Pan, M. H.; Gao, J. H.; Lai, C. S.; Wang, Y. J.; Chen, W. M.; Lo, C. Y.; Wang, M.; Dushenkov, S.; Ho, C. T. Antitumor activity of 3,5,4′-trimethoxystilbene in COLO 205 cells and xenografts in SCID mice. *Mol. Carcinog.* **2008**, *47* (3), 184–196.

(17) Lu, J.; Ho, C. H.; Ghai, G.; Chen, K. Y. Resveratrol analog, 3,4,5,4′-tetrahydroxystilbene, differentially induces pro-apoptotic p53/Bax gene expression and inhibits the growth of transformed cells but not their normal counterparts. *Carcinogenesis* **2001**, *22* (2), 321–328.

(18) Agarwal, C.; Dhanalakshmi, S.; Singh, R. P.; Agarwal, R. Inositol hexaphosphate inhibits growth and induces G1 arrest and apoptotic death of androgen-dependent human prostate carcinoma LNCaP cells. *Neoplasia* **2004**, *6* (5), 646–659.

(19) el-Deiry, W. S.; Harper, J. W.; O'Connor, P. M.; Velculescu, V. E.; Canman, C. E.; Jackman, J.; Pietenpol, J. A.; Burrell, M.; Hill, D. E.;

Wang, Y.; et al. WAF1/CIP1 is induced in p53-mediated G1 arrest and apoptosis. *Cancer Res*. **1994**, *54* (5), 1169–1174.
(20) Parker, S. B.; Eichele, G.; Zhang, P.; Rawls, A.; Sands, A. T.; Bradley, A.; Olson, E. N.; Harper, J. W.; Elledge, S. J. p53-independent expression of p21Cip1 in muscle and other terminally differentiating cells. *Science* **1995**, *267* (5200), 1024–1027.
(21) Tolomeo, M.; Grimaudo, S.; Di Cristina, A.; Roberti, M.; Pizzirani, D.; Meli, M.; Dusonchet, L.; Gebbia, N.; Abbadessa, V.; Crosta, L.; Barucchello, R.; Grisolia, G.; Invidiata, F.; Simoni, D. Pterostilbene and 3′-hydroxypterostilbene are effective apoptosis-inducing agents in MDR and BCR-ABL-expressing leukemia cells. *Int*. *J*. *Biochem*. *Cell Biol*. **2005**, *37* (8), 1709–1726.
(22) Simoni, D.; Roberti, M.; Invidiata, F. P.; Aiello, E.; Aiello, S.; Marchetti, P.; Baruchello, R.; Eleopra, M.; Di Cristina, A.; Grimaudo, S.; Gebbia, N.; Crosta, L.; Dieli, F.; Tolomeo, M. Stilbene-based anticancer agents: resveratrol analogues active toward HL60 leukemic cells with a non-specific phase mechanism. *Bioorg*. *Med*. *Chem*. *Lett*. **2006**, *16* (12), 3245–3248.
(23) Ma, Z.; Molavi, O.; Haddadi, A.; Lai, R.; Gossage, R. A.; Lavasanifar, A. Resveratrol analog trans 3,4,5,4′-tetramethoxystilbene (DMU-212) mediates anti-tumor effects via mechanism different from that of resveratrol. *Cancer Chemother*. *Pharmacol*. **2008**, *63* (1), 27–35.
(24) Wang, C.; Li, Z.; Fu, M.; Bouras, T.; Pestell, R. G. Signal transduction mediated by cyclin D1: from mitogens to cell proliferation: a molecular target with therapeutic potential. *Cancer Treat*. *Res*. **2004**, *119*, 217–237.
(25) Kim, A. L.; Zhu, Y.; Zhu, H.; Han, L.; Kopelovich, L.; Bickers, D. R.; Athar, M. Resveratrol inhibits proliferation of human epidermoid carcinoma A431 cells by modulating MEK1 and AP-1 signalling pathways. *Exp*. *Dermatol*. **2006**, *15* (7), 538–546.
(26) Gladden, A. B.; Diehl, J. A. Location, location, location: the role of cyclin D1 nuclear localization in cancer. *J*. *Cell Biochem*. **2005**, *96* (5), 906–913.
(27) Kelly-Spratt, K. S.; Philipp-Staheli, J.; Gurley, K. E.; Hoon-Kim, K.; Knoblaugh, S.; Kemp, C. J. Inhibition of PI-3K restores nuclear p27(Kip1) expression in a mouse model of Kras-driven lung cancer. *Oncogene* **2009**, *28* (41), 3652–3662.
(28) McLean, G. W.; Carragher, N. O.; Avizienyte, E.; Evans, J.; Brunton, V. G.; Frame, M. C. The role of focal-adhesion kinase in cancer − a new therapeutic opportunity. *Nat*. *Rev*. *Cancer* **2005**, *5* (7), 505–515.
(29) Li, S.; Hua, Z. C. FAK expression regulation and therapeutic potential. *Adv*. *Cancer Res*. **2008**, *101*, 45–61.
(30) Brunton, V. G.; Frame, M. C. Src and focal adhesion kinase as therapeutic targets in cancer. *Curr*. *Opin*. *Pharmacol*. **2008**, *8* (4), 427–432.

**Received for review September 2, 2009. Revised manuscript received October 15, 2009. Accepted November 6, 2009. This study was supported by the National Science Council (Grants NSC 96-2320-B-040-023 and NSC 97-2320-B-040-015-MY3).**